

## Groove model of tibia-femoral osteoarthritis in the rat

de Visser, H.M.; Weinans, Harrie; Coeleveld, K.; van Rijen, M.H.P.; Lafeber, F.P.J.G.; Mastbergen, S.C.

**DOI**

[10.1002/jor.23299](https://doi.org/10.1002/jor.23299)

**Publication date**

2016

**Document Version**

Final published version

**Published in**

Journal of Orthopaedic Research: a journal for musculoskeletal investigation

**Citation (APA)**

de Visser, H. M., Weinans, H., Coeleveld, K., van Rijen, M. H. P., Lafeber, F. P. J. G., & Mastbergen, S. C. (2016). Groove model of tibia-femoral osteoarthritis in the rat. *Journal of Orthopaedic Research: a journal for musculoskeletal investigation*, 35 (2017)(3), 496-505. <https://doi.org/10.1002/jor.23299>

**Important note**

To cite this publication, please use the final published version (if applicable). Please check the document version above.

**Copyright**

Other than for strictly personal use, it is not permitted to download, forward or distribute the text or part of it, without the consent of the author(s) and/or copyright holder(s), unless the work is under an open content license such as Creative Commons.

**Takedown policy**

Please contact us and provide details if you believe this document breaches copyrights. We will remove access to the work immediately and investigate your claim.

# Groove Model of Tibia-Femoral Osteoarthritis in the Rat

Huub M. de Visser,<sup>1,2</sup> Harrie Weinans,<sup>1,2,3</sup> Katja Coeleveld,<sup>1</sup> Mattie H. P. van Rijen,<sup>2</sup> Floris P. J. G. Lafeber,<sup>1</sup> Simon C. Mastbergen<sup>1</sup>

<sup>1</sup>Department of Rheumatology and Clinical Immunology, University Medical Center Utrecht, UMC Utrecht, F.02.127, P.O. Box 85500, 3508 GA Utrecht, The Netherlands, <sup>2</sup>Department of Orthopaedics, University Medical Center Utrecht, Utrecht, The Netherlands, <sup>3</sup>Department of Biomechanical Engineering, Delft University of Technology, Delft, The Netherlands

Received 2 February 2016; accepted 6 May 2016

Published online in Wiley Online Library (wileyonlinelibrary.com). DOI 10.1002/jor.23299

**ABSTRACT:** Several experimental models of osteoarthritis in rats are used to study the pathophysiology of osteoarthritis. Many mechanically induced models have the limitation that permanent joint instability is induced by, for example, ligament transection or meniscal damage. This permanent instability will counteract the potential beneficial effects of therapy. The groove model of osteoarthritis uses a one-time trigger, surgically induced cartilage damage on the femoral condyles, and has been validated for the canine tibia-femoral compartment. The present study evaluates this model for the rat knee joint. The articular cartilage of the weight bearing surface of both femoral condyles and trochlea were damaged (grooved) without damaging the underlying subchondral bone. Severity of joint degeneration was histologically assessed, in addition to patella cartilage damage, and subchondral bone characteristics by means of (contrast-enhanced) micro-CT. Mild histological degeneration of the surgically untouched tibial plateau cartilage was observed in addition to damage of the femoral condyles, without clear synovial tissue inflammation. Contrast enhanced micro-CT demonstrated proteoglycan loss of the surgically untouched patella cartilage. Besides, a more sclerotic structure of the subchondral bone was observed. The tibia-femoral groove model in a rat results in mild knee joint degeneration, without permanent joint instability and joint inflammation. This makes the rat groove model a useful model to study the onset and progression of post-traumatic non-inflammatory osteoarthritis, creating a relatively sensitive model to study disease modifying osteoarthritic drugs. © 2016 The Authors. *Journal of Orthopaedic Research* published by Wiley Periodicals, Inc. on behalf of the Orthopaedic Research Society. *J Orthop Res*

**Keywords:** osteoarthritis; OA animal model; rat; cartilage; bone

Osteoarthritis (OA) is the most prevalent chronic joint disorder with pain and loss of function as main clinical features.<sup>1</sup> In principle, OA is slowly progressing and increases in prevalence and severity with increasing age.<sup>2</sup> The complex pathogenic changes in human OA can take several decades to develop and may be influenced by a multitude of factors, including predisposing factors that contribute during the process of OA development, that is, genetics, hormonal status, and body mass.<sup>3</sup> The disease involves not only articular cartilage as is frequently studied, but the whole joint, including subchondral bone, synovial tissue, capsule, ligaments, and muscles.<sup>4</sup>

Studies of OA in humans are restricted by the slow rate at which the disease progresses and the limited opportunity to study the tissue changes over time. Moreover, the diagnosis of OA is still established late in the disease process, and disease modifying treatments are still unavailable.<sup>5</sup> So far only surrogate markers (biochemical and imaging) with limited discriminating strength are available.<sup>6</sup> As such, the

problem of the lack of good correlation between the clinical features and pathology remains. The need to clarify the molecular pathogenic events that occur in various joint tissues at the onset and during the progression of OA has therefore urged the use of models that can exhibit the relevant features that characterize the human disease. To understand the complex inter-relationship between the different disease mechanisms, joint tissues, and body systems, studying OA in animal models can help to elucidate the complex mechanistic aspects of OA.

Spontaneous OA development, similar to the human situation, has been reported for a few laboratory animal species,<sup>7–9</sup> although the disease development in these animals proceeds slowly and specific predisposing genetics may underlie these models.<sup>10,11</sup> In rats, the occurrence of spontaneous OA development is rare.<sup>12</sup> To induce OA in rats, several experimental models are used, either surgical or chemical induced and also non-invasive loading models, to study OA pathophysiology and its potential treatment.<sup>13–17</sup> The mechanically induced models, such as the frequently used anterior cruciate ligament transection (ACLT<sup>14</sup>) and destabilization of the medial meniscus (DMM<sup>18</sup>), have the limitation that they induce a permanent trigger during the course of OA, namely instability, counteracting the potential beneficial effects of therapy. This makes these models less suitable for studying disease modifying OA drug therapies.<sup>10</sup>

Models without a permanent trigger have been described and are expectedly more sensitive to therapy.<sup>19,20</sup> A well-validated example of such a model is the canine groove model of joint degeneration, with features of joint degeneration mimicking early human

This is an open access article under the terms of the Creative Commons Attribution-NonCommercial-NoDerivs License, which permits use and distribution in any medium, provided the original work is properly cited, the use is non-commercial and no modifications or adaptations are made.

Conflicts of interest: None.

Grant sponsor: European Union Seventh Framework Programme (FP7/2007–2013); Grant number: n°305815; Grant sponsor: Dutch Arthritis Foundation; Grant number: LLP-22; Grant sponsor: Health–Holland.

Correspondence to: Simon C. Mastbergen (T: +31-88-7559758; F: +31-88-7555639; E-mail: S.Mastbergen@umcutrecht.nl)

© 2016 The Authors. *Journal of Orthopaedic Research* published by Wiley Periodicals, Inc. on behalf of the Orthopaedic Research Society.

OA.<sup>19,21–24</sup> In this large animal model, damage of the articular cartilage of the weight-bearing areas of the femoral condyles is the trigger for development of joint changes consistent with early OA. This model is characterized by slowly progressive cartilage damage, subchondral bone changes, mild inflammation, and pain as observed by force plate analysis.<sup>25</sup> Although the dog has good kinematics for translation to the human situation, and is relatively large to perform a multitude of tissue tests including biochemical analyses of cartilage, important drawbacks of this model are cost, smaller availability of facilities for housing, duration of the experiments, and ethical concerns. This tempted us to evaluate this model in a smaller animal.

Derivatives of the groove models have been described for rats in literature.<sup>26–28</sup> However, these models are not optimal as they either create a full-thickness cartilage defect, which damages the underlying subchondral bone,<sup>27,28</sup> or only damage the non-weight bearing cartilage of the femoral trochlea, resulting in patella-femoral joint degeneration only.<sup>26</sup> Given tibia-femoral OA is the most prevalent type of post-traumatic knee OA, and the available models do not induce local cartilage damage in this compartment, we translated the canine groove model to the rat. We created a modified surgical model, inducing intrinsic cartilage damage on the weight bearing surface of the femoral condyles in addition to the femoral trochlea, and evaluated the subsequent knee joint degeneration throughout the entire joint.

## METHODS

### Study Design

Ten male Wistar rats (523 ± 44 g, Charles-River, Sulzfeld, Germany), 16 weeks of age, were housed, two per cage, in a 12:12 light-dark cycle (light-on period, 7:00 AM–7:00 PM). All animals had access to standard food pellets and tap water ad libitum. An overview of the study set-up is given in Figure 1. All procedures were approved by the Utrecht University Medical Ethical Committee for animal studies (DEC 2014. III.05.049) and ARRIVE guidelines were fully complied.

### Surgical Procedure

In all rats ( $n = 10$ ), surgery was performed in the right knee joint at baseline, under general anesthesia (Isofluran), to induce local cartilage damage as indicated in Figure 2. The knee joint cavity was opened with a small longitudinal incision through the *ligamentum patellae* of the right knee joint. The tip of an enhanced surgical tool was bent 90° at

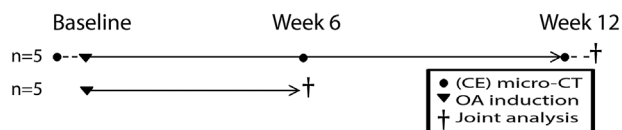


**Figure 1.** Experimental design of the study where OA induction is performed by groove surgery in ten 16-week-old male Wistar rats. At baseline, prior to surgery, 6 and 12 weeks ( $n = 5$ ) after OA induction contrast enhanced micro-CT was performed. One group was euthanized at 6 weeks to evaluate joint damage by histology, the other group continued for another 6 weeks before euthanization to evaluate joint damage.

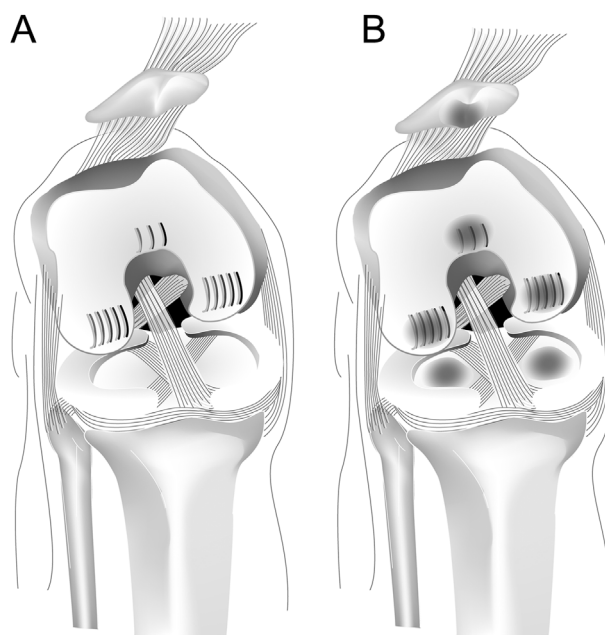


**Figure 2.** Schematic location of grooves placed on the weight bearing surface of the articular cartilage of both femoral condyles and the femoral trochlea (A). Schematic overview of the hypothetical location of subsequent joint degeneration (B).

150–180  $\mu\text{m}$  from the tip, to ensure not to damage the underlying subchondral bone, as the articular cartilage of a rat is approximately 200–250  $\mu\text{m}$  thick.<sup>26</sup> With this surgical tool we applied five longitudinal grooves on the weight bearing area of the articular cartilage of both the medial and lateral femoral condyle, while the knee joint was flexed to the utmost position. This was done in addition to three longitudinal grooves on the non-weight bearing surface of the articular cartilage of the femoral trochlea, according to Siebelt et al.<sup>26</sup> (see Fig. 2). The opposite articular cartilage of the tibial compartment was not surgically damaged, the same applies to the patellar cartilage. The contralateral non-operated left knee joint served as internal control. After the surgical procedure, all animals were immediately allowed to move freely and no joint instability was observed. Analgesia (Buprenorphine 0.05 mg/kg) was submitted subcutaneously until 24 h after surgery. All animals quickly recovered after surgery and no wound healing problems were observed.

### Patella Cartilage Evaluation With Contrast Enhanced Micro-CT

At baseline animals were randomly divided in two groups (see Fig. 1). One group was euthanized at 6 weeks to evaluate joint damage by histology, the other group continued for another 6 weeks before euthanization. In the latter group, at baseline, prior to surgery, 6 and 12 weeks ( $n = 5$ ) after induction of joint damage contrast enhanced micro-CT ( $\mu\text{-CT}$ ), using a Quatum FX  $\mu\text{-CT}$  scanner (PerkinElmer, Waltham, MA) was performed under isoflurane sedation to measure in vivo patellar cartilage thickness and attenuation. This method is validated for the patellar cartilage, but not for the femoral and tibial cartilage, in rats.<sup>26,29</sup> Hexabrix320 (Guerbet, Gorinchem, The Netherlands) was used as contrast agent. Hexabrix is a 600 mOsm, radio-opaque, solution of the salts ioxaglate-meglumine, and ioxaglate-sodium. The contrast agent is already applied in vivo in humans and no acute toxic effects in rats are reported.<sup>29–31</sup> Due to the negative fixed

charged density of the cartilage, as a result from the local glucosaminoglycan (GAG) content, the negatively charged ioxglate will be locally repulsed. Whereby, ioxglate penetration results in a concentration inversely related to the cartilage sulfated-glycosaminoglycan (sGAG) content and thereby indicative of tissue quality.<sup>32,33</sup> An amount of 75  $\mu$ l non-diluted Hexabrix320 was mixed with 0.75  $\mu$ g Epinephrine (Centrafarm, Etten-Leur, The Netherlands) to induce adequate vasoconstriction and thereby prevent leakage of ioxglate out of the knee joint cavity.<sup>29,34</sup> The Hexabrix/Epinephrine mixture was injected into the grooved knee joint cavity at a very slow pace (15 s), using a 27 Gauche needle (Sherwood-Davis & Geck, UK), with the knee in slight flexion. Immediately after injection, the joint was slowly mobilized passively for adequate distribution of the Hexabrix320 throughout the knee joint cavity. Five minutes after injection the rat was transferred into a holder in supine position and the hind legs fixated in extension. Subsequently, the grooved knee joints were in vivo scanned with  $\mu$ -CT. The  $\mu$ -CT scans were made using a 3 min scan per knee joint at an isotropic voxel size of 21  $\mu$ m, at a voltage of 90 kV, a current of 180 UA, field of view of 42 mm. All scans were identically performed and reconstructed using the Quatum FX  $\mu$ -CT scanner, post-processing of the images is performed by Analyze (PerkinElmar). For articular cartilage analysis of the patellofemoral joint, in all contrast enhanced- $\mu$ CT datasets, X-ray attenuation (arbitrary gray values inversely related to sGAG content), and cartilage thickness ( $\mu$ m) of the patella was calculated, using ImageJ software (ImageJ) from standardized regions of interest (ROI) for a total of 20 slides.

#### Subchondral Bone Evaluated by Micro-CT

To evaluate subchondral bone changes,  $\mu$ -CT data from baseline and 12 weeks follow-up were subjected to a  $\mu$ CT evaluation of subchondral bone changes. The  $\mu$ -CT scans were made using a 3 min scan per knee joint at an isotropic voxel size of 21  $\mu$ m, at a voltage of 90 kV, a current of 180 UA, field of view of 42 mm. All scans were identically performed and reconstructed using the Quatum FX  $\mu$ -CT scanner, post-processing of the images is performed by Analyze (PerkinElmar). Using ImageJ software (ImageJ) the regions of interest (ROI) were standardized, by starting in the back of the knee joint from the point where the medial and lateral compartments of the tibial epiphysis unite for a total of 90 slides onwards to the front of the knee joint. Bone was segmented from the  $\mu$ -CT datasets in coronal orientation with a local threshold algorithm (Bernsen, radius 5) from the coronal sections.<sup>35</sup> Subsequently, the ROI's of the tibial epiphysis were manually drawn for the mean subchondral plate thickness ( $\mu$ m), the mean trabecular bone thickness ( $\mu$ m) and trabecular bone volume fraction (BV/TV), representing the ratio of trabecular bone volume (BV, in  $\text{mm}^3$ ) to endocortical tissue volume (TV, in  $\text{mm}^3$ ) and the data for the medial and lateral side was averaged. In addition, all outcome parameters were also separated for the medial and lateral compartment of the tibia plateau. To control for normal growth related subchondral bone changes, retrospective data from strain and age matched healthy control knee joints were used to determine groove unrelated subchondral bone changes between baseline and 12 weeks post-surgery.

#### Histopathological Examination of the Knee Joint

Animals were euthanized either 6 ( $n = 5$ ) or 12 ( $n = 5$ ) weeks after OA induction, and whole joint degeneration was evaluated using the OARSI histopathology score for rats.<sup>12</sup> The

histological preparations were performed according to the guidelines.<sup>12</sup> All knee joints were fixed in 3.8% phosphate buffered formaldehyde for 3 days and subsequently decalcified with EDTA (12,5%) for a period of 21 days. The decalcified tissue was dehydrated via 70–100% ethanol, rinsed in xylene and finally embedded in paraffin. Coronal sections of 5  $\mu$ m thickness were made at 100  $\mu$ m intervals and stained with Hematoxylin & Eosin (H&E) to determine the degree of synovial membrane inflammation and Safranin-O (Saf-O) with a fast green counterstain to envision the amount and distribution of the GAGs. The parameters of the histologic scoring includes cartilage matrix loss width, cartilage degeneration, cartilage degeneration width, osteophytes, synovial reaction and calcified cartilage, and subchondral bone damage.<sup>12</sup> Only tibia-femoral cartilage is assessed as coronal sectioning obtains optimally oriented mid-coronal sections, making this less suitable for patellar cartilage evaluation.<sup>12</sup> The placed grooves itself were not taken into account, only the direct adjacent cartilage to study the effect of the model. Assessment of joint degeneration is performed in random order, independently by two observers unaware of the source of the samples.

#### Statistical Analysis

Histological data is presented for both knee joints of each animal separately, as well as mean values with 95% confidence interval of five animals in each group. Comparison between grooved experimental and contralateral control knee joints was performed by the Wilcoxon signed ranks test. Comparison between the grooved experimental joints at 6 and 12 weeks was performed by Mann-Whitney *U* test. Patella cartilage from contrast enhanced  $\mu$ -CT data are presented as means with 95% confidence interval and comparisons between the different time points was performed by the paired samples *t*-test. All subchondral bone changes originated from  $\mu$ -CT imaging are presented as mean with 95% confidence interval to analyze differences between the experimental knee joints and healthy control knee joints the independent samples *t*-test was used. Comparison between the grooved experimental and contralateral control knee joints was performed by the paired samples *t*-test. (SPSS statistics 21, SPSS inc., Chicago, IL) For all tests *p* values <0.05 were considered statistically significant different.

## RESULTS

### Histopathological Joint Degeneration

In order to validate the groove model, an OA model based on a one-time trigger, in the rat we performed a feasibility study with 6 and 12 week follow-up.

Inducing local cartilage damage on the femoral condyles and trochlea by groove surgery in rat knee joints resulted in statistically significant higher, although still mild, whole joint degeneration compared to the contralateral control knee joint at both 6- and 12-weeks post-surgery (Fig. 3A and E). Synovial membrane inflammation scores (a parameter of the total OARSI score) in the surgically damaged knee joints were all relatively small and did not show any differences compared to the unoperated contralateral control knee joints (Fig. 3B and E). The most pronounced difference between the grooved and the contralateral control knee joints is observed on the

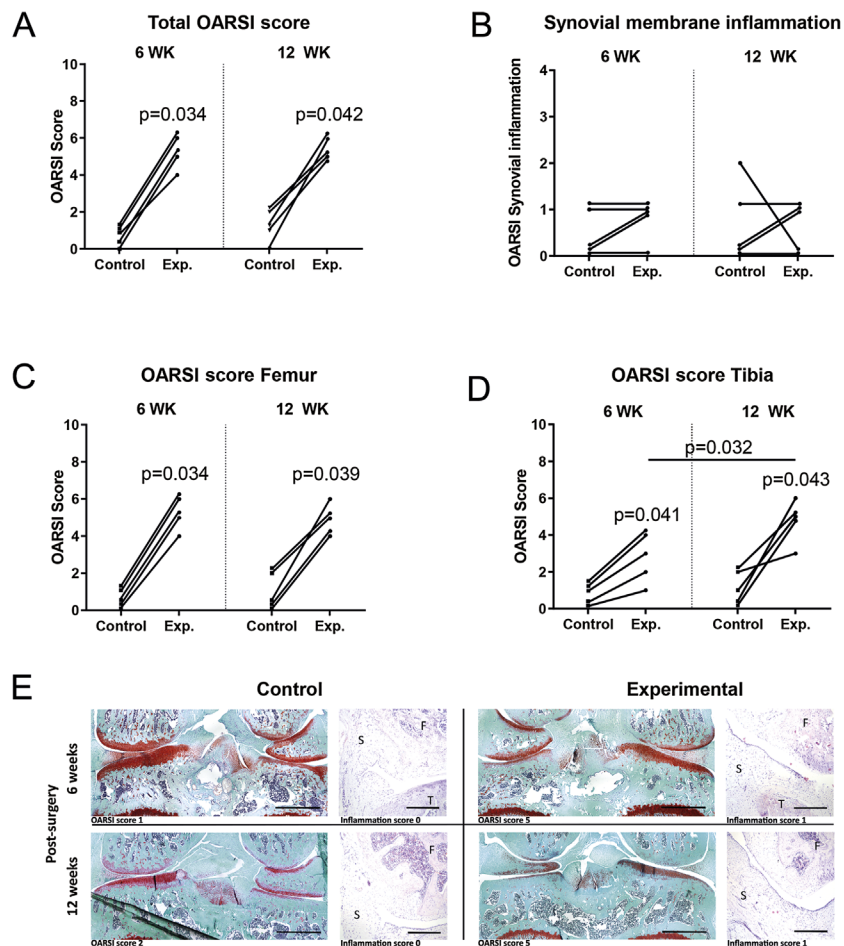


**Figure 3.** Histological changes in joint degeneration as a result of experimentally induced joint damage on the femoral condyles in the rat knee joint, values are presented for OARSI score of control and experimental (Exp.) knee joints. Individual changes for total joint degeneration (A), synovial membrane inflammation score (a parameter of the total OARSI score; B), joint degeneration of the femur (C) and tibia (D) separately, 6 weeks (left) and 12 weeks post-surgery (right) are shown. *p* values indicates statistical significant changes compared to contralateral controls with a Wilcoxon signed ranks test and changes between 6 and 12 weeks post-surgery with the Mann–Whitney *U* test. Representative light micrographs from Safranin-O (Saf-O) staining of rat knee joints and Hematoxylin & Eosin (H&E) staining for synovial membrane inflammation 6- and 12-weeks post-surgery are presented (E). In the H&E images F, femur; T, tibia, and S, synovial membrane. Scale bar of Saf-O staining is 1 mm and H&E staining is 200  $\mu$ m.

articular cartilage of the surgically damaged femoral condyles. Change at the femoral condyles was clearly found direct adjacent to the grooves 6 weeks post-surgery, with no further increase of cartilage degeneration at 12-weeks post-surgery (Fig. 3C). More interesting, the tibia plateau, not surgically damaged, demonstrated a statistically significant increase in articular cartilage degeneration compared to the tibia plateau of the contralateral control knee joints in all animals (Fig. 3D). When the amount of articular cartilage degeneration of the tibia in the grooved knee joints at 12-weeks post-surgery is compared to 6-weeks post-surgery the articular cartilage degeneration is even further increased (Fig. 3D).

When looking specifically to the medial and lateral side of the articular cartilage, we found a considerable increase in joint degeneration in both compartments of the femoral condyles, compared to the contralateral control knee joints (Fig. 4A, B, and E). On the tibia plateau, the medial side had a relatively mild degener-

ation of the articular cartilage compared to the contralateral control knee joints (Fig. 4C and E). The lateral side on the other hand, showed more severe articular cartilage degeneration in the operated knee joints compared to the contralateral control knee joints. This increase in degeneration on the tibia plateau is mainly caused by the increased articular cartilage degeneration in the grooved knee joints 12-weeks post-surgery compared to 6-weeks post-surgery (Fig. 4D and E).

#### Patellar Cartilage Changes

As measured from the ROI of contrast enhanced  $\mu$ -CT scans, 6 and 12 weeks after induction of the local cartilage damage, the thickness of the surgically untouched patellar cartilage decreased over time (Fig. 5A).

Whereas the gray value (representing the inverse relation to the cartilage GAG content) of the patellar cartilage increased over time (Fig. 5B).

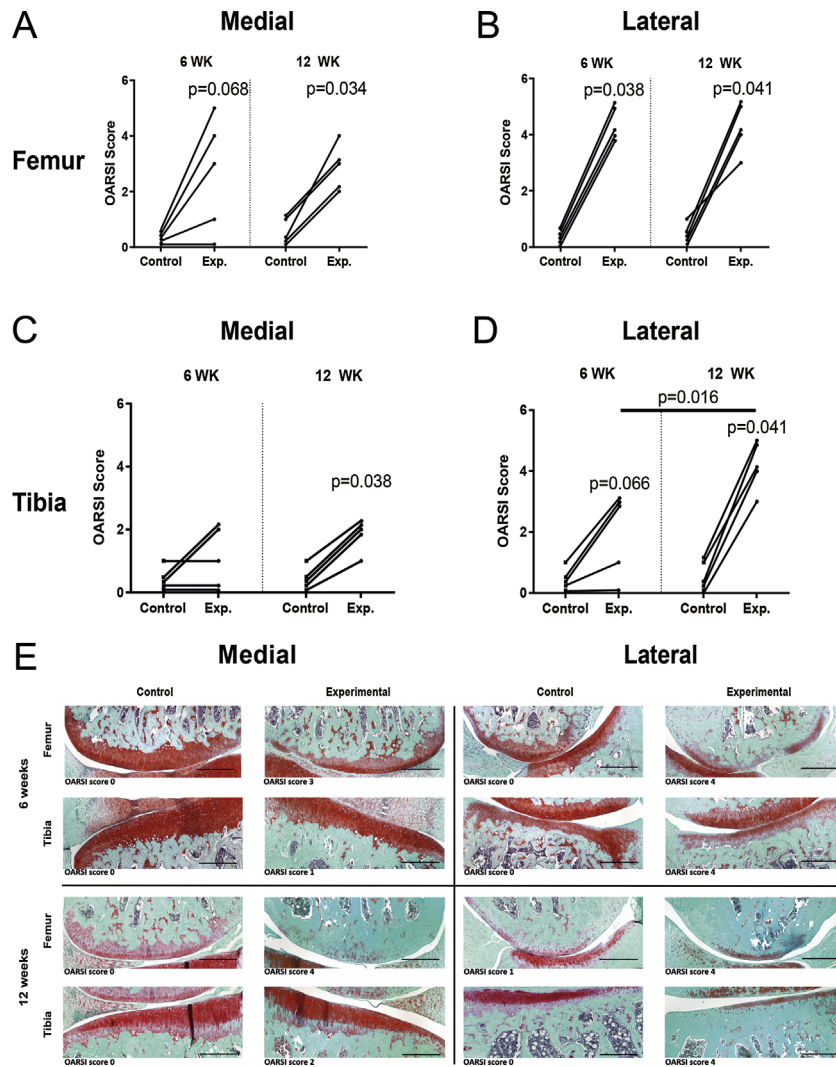


**Figure 4.** Joint location specific individual changes of the OARSI histopathology score on the femur (A and B) and surgically untouched tibia (C and D) separated for the medial (A and C) and the lateral (B and D) side 6-weeks post-surgery and 12-weeks post-surgery. Values are presented for control and experimental (Exp.) knee joints of individual animals. *p* values indicates statistical changes compared to contralateral controls with a Wilcoxon signed ranks test and changes between 6- and 12-weeks post-surgery with the Mann–Whitney *U* test. Representative images from Safranin-O (Saf-O) stained histological sections from the joint specific locations of the femoral and tibia plateau cartilage after 6 weeks and 12 weeks of groove surgery on the medial and lateral side. (E) Scale bar of Saf-O staining is 200  $\mu$ m.

### Subchondral Bone Changes

By  $\mu$ -CT imaging, all subchondral bone parameters, which originated from the untouched tibia compartment of the knee joints, increased over time. A statistical significant increase was found for the subchondral plate thickness (+9.5%), trabecular bone thickness (+16.3%), and trabecular bone volume (+16.3%) compared to their baseline measurements, indicating a more sclerotic structure as seen in human OA. (Left panels of Fig. 6B–D; WK12) When comparing the subchondral bone parameters of the experimental knee joints with healthy control knee joints 12-weeks post-surgery the groove related bone changes were increased for subchondral plate thickness, trabecular bone thickness, and trabecular bone volume (Left panels of Fig. 6B–D; Control vs. WK12). Looking more closely to the subchondral bone differences on

the tibia, the medial and lateral side of the subchondral bone were separated. For both the medial and the lateral sides all parameters were increased compared to baseline measurements in the grooved knee joints (Middle and right panels of Fig. 6B–D; WK12). Only trabecular bone parameters, and not subchondral plate, were increased on both the medial and lateral side in the experimental knee joints compared to healthy control joints (Middle and right panels of Fig. 6B–D; Control vs. WK 12). Osteophyte formation, easily detectable by  $\mu$ -CT, was not seen within the entire joint of both the experimental and the control knee joints of all rats.

### DISCUSSION

This study demonstrates that the groove model of local femoral cartilage damage in the rat, leads to early

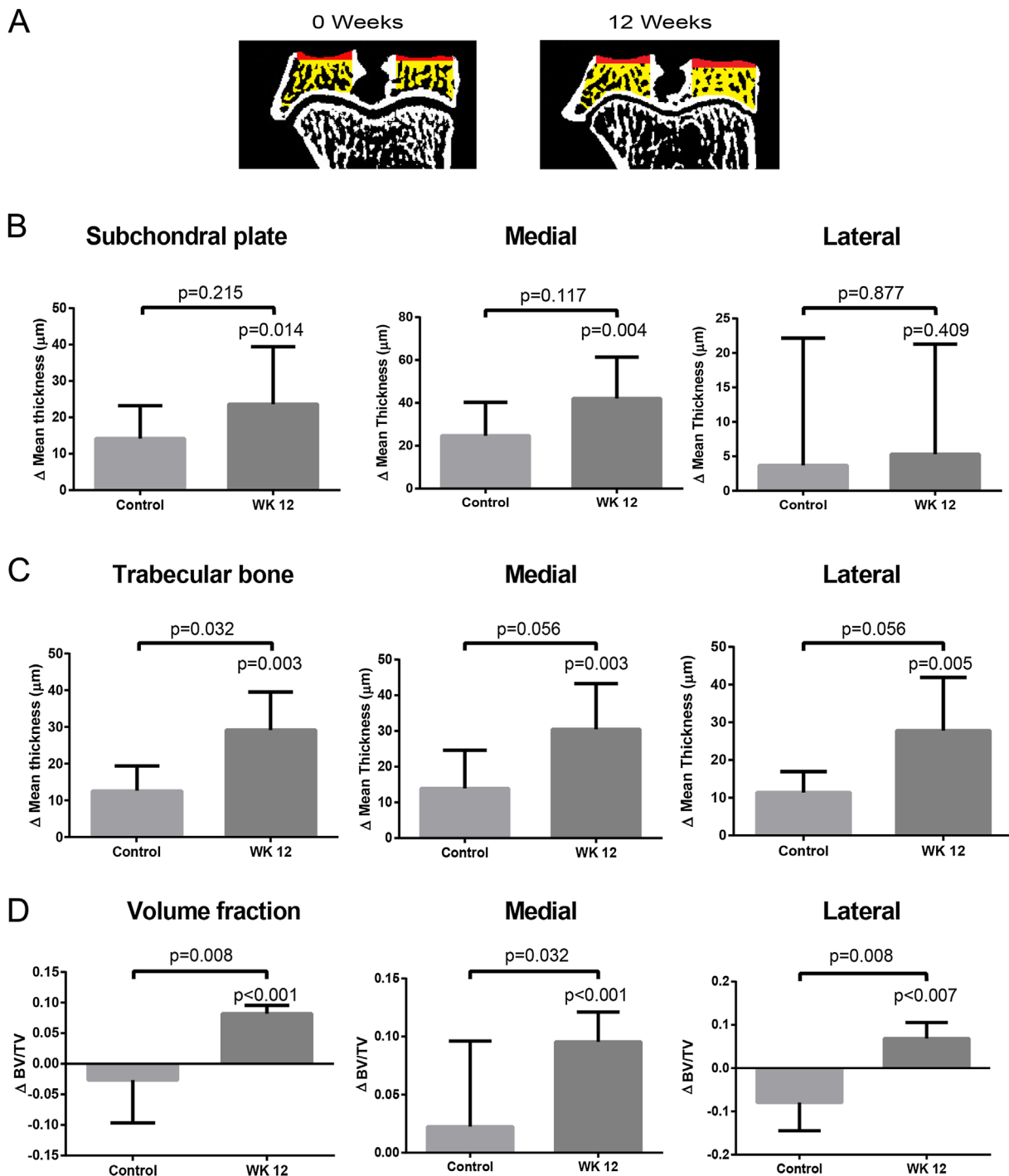


**Figure 5.** Representative in vivo micro-CT-arthrography scans of the patella cartilage at baseline, 6- and 12-weeks after surgical applied cartilage damage on the opposite femoral trochlea. Groove surgery on the femoral trochlea resulted in a decrease of patellar cartilage thickness (A) and an increase of cartilage attenuation, which is inversely related to sGAG content, indicating impaired articular cartilage quantity and quality 6 and 12 weeks post-surgery (B). Bars represent mean with 95% confidence interval of  $n = 5$  animals.  $p$ -value indicates statistical significant changes compared to baseline measurements with paired samples  $t$ -test.

degenerative joint changes with slow onset, in both the directly damaged (femoral condyles and trochlea) as the opposite (untouched tibia and patella) joint compartments. A distinctive difference with other surgical rat models of OA is the lack of destabilization which is a persistent trigger causing joint damage. Furthermore, the model does not induce inflammation

and osteophyte formation, hereby mimicking (early) human OA development. Damaging the articular cartilage without damage to the direct underlying subchondral bone is an important aspect of the groove model, as bone damage can result in release of precursor cells with reparative characteristics influencing the disease development.<sup>36</sup> A first adaptation of

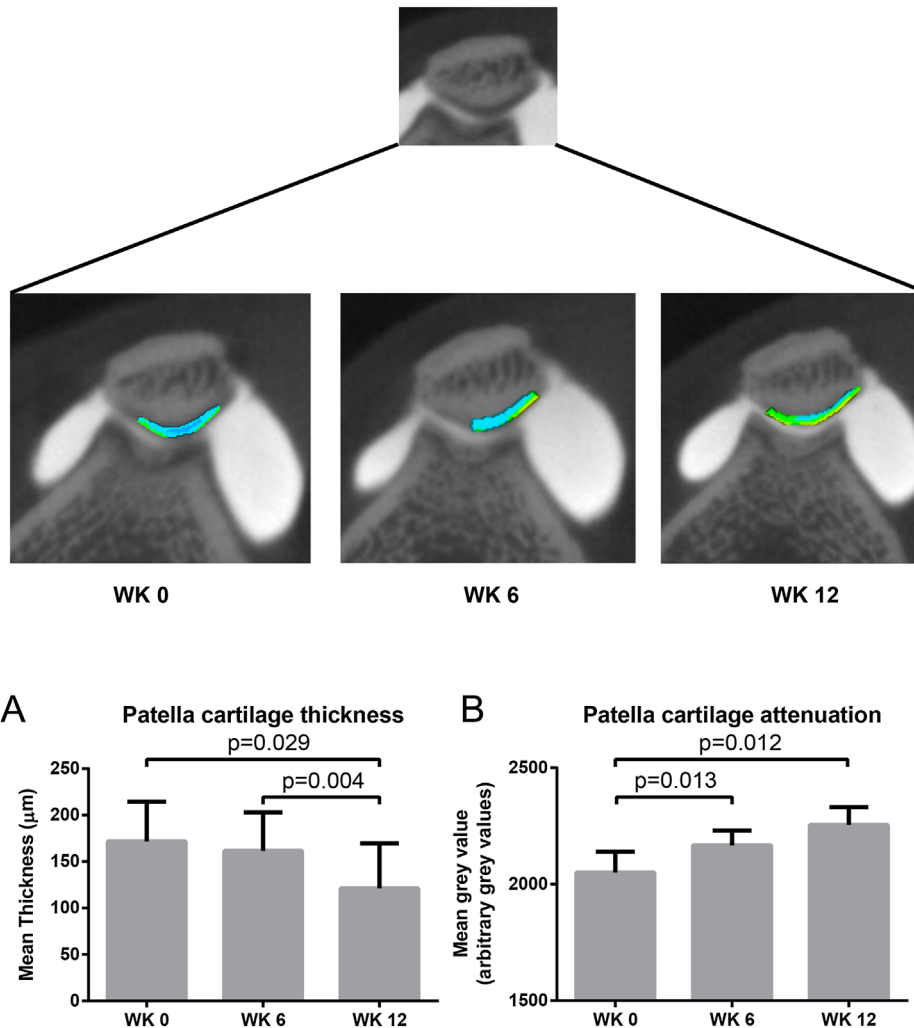


**Figure 6.** Representative micro-CT reconstruction of the surgically untouched tibia compartment. The subchondral plate thickness is derived from the area marked in red and the trabecular bone thickness and volume fraction from the yellow marked area. (A). The average delta change between baseline and 12 week physiological bone changes in healthy controls (Control) and between baseline and 12 weeks post-surgery (WK12) of the subchondral plate thickness (B; left), trabecular bone thickness (C; left) and bone volume fraction (D; left) are shown. In more detail the change over time of all subchondral bone parameters, separated for the medial B–D; middle and lateral (B–D; right) side of the tibia compartment are given. Bars represent mean change with 95% confidence interval of  $n = 5$  animals.  $p$ -value indicates statistical changes compared to baseline measurements with paired samples  $t$ -test and compared to healthy joints from age-matched control rats with independent samples  $t$ -test.

the groove model in the rat is previously described by Siebelt et al.,<sup>26</sup> where only the non-weight bearing femoral trochlea was grooved and subsequently only local cartilage degeneration in the patellofemoral compartment was observed. To achieve whole joint degeneration we attempt to damage the articular cartilage on the weight bearing area of the femoral condyles, similar as the original canine groove model.<sup>19,22</sup> Therefore, the surgical procedure previously described by Siebelt et al.<sup>26</sup> was modified and the weight bearing surface of both femoral condyles as well as the femoral trochlea were grooved without extending the incision. The limitation of this rat groove model compared to the canine groove model is the limited freedom of movement during the microsurgical procedure and the lack of visual confirmation applying the grooves at the articular cartilage. Despite the difficult microsurgical procedure, analysis of

histopathological sections confirmed the surgical applied cartilage damage without scratching the direct underlying subchondral bone. Quantitatively similar effects were found in all experimental knee joints. This indicates that although standardization of the location of the placed grooves has its restrictions, the results obtained are highly reproducible.

A big advantage of using a small animal, such as a rat, as a model for OA research is the possibility to monitor in vivo the disease process longitudinally with  $\mu$ -CT. However, mice, due to their small size, are not ideal for this model with the complex microsurgery. Besides the cartilage of mice knee joints has relatively few cell layers and a reduced zonal tissue organization as compared to larger species and is therefore as a model less ideal to study the alterations of the biomechanical function of the joint.<sup>37</sup> Rats, unlike mice, possess a thicker cartilage with a complex zonal



structure, more comparable to the human structure, which makes partial and full-thickness cartilage lesions reproducible.<sup>12</sup> The rat groove model has its limitations compared to the larger animals as biochemical changes, pain evaluations by force plate analysis and synovial fluid sampling are difficult due to the size of the animal and the knee joint. Another limitation of a rat animal model is the thin cartilage, which might be easier to repair than human articular cartilage.<sup>38</sup> Furthermore, still little is known how closely a therapeutic effect in a rat model will mirror therapeutic activity in man.<sup>39</sup>

In this rat groove model, the contralateral rat knee joint is not been sham operated on, Siebelt et al.<sup>26</sup> performed a sham surgery and did not see any difference in synovial inflammation and cartilage degeneration 12 weeks after sham surgery compared to non-operated control rat knee joints in rats of the same strain and age. Moreover, sham surgery performed in canine knee joints, a more extensive procedure compared to the rat, demonstrated no effect of the surgery compared to non-operated canine knee joints.<sup>19,24,40</sup> Based on these previous results, we anticipate no difference between sham surgery and non-operated control knee joints. As such we consider the non-operated contralateral leg as an internal control.

The histological changes found in this rat groove model were most pronounced on the femoral condyles. Although the placed grooves itself were not taken into account in the scoring, we demonstrated an enhanced degeneration indicating that the placed grooves affects the direct adjacent cartilage, already 6-weeks post-surgery. For the tibia plateau on the other hand, degeneration of the articular cartilage continues to progress up to 12-weeks post-surgery. The OA related degenerative changes of the tibia plateau do not solely occur on the articular cartilage, directly opposite the grooved cartilage of the femur, but also on the underlying subchondral bone of the untouched tibial compartment 12-weeks post-surgery. These changes might be caused by the natural growth of rats as this affects the subchondral bone. Although we used skeletally mature rats,<sup>12</sup> the rats will continue growing as the growth plate closes at approximately 8 months of age.<sup>41</sup> To control for normal growth related subchondral bone changes, healthy control knee joints were used to determine groove unrelated subchondral bone changes. Taken into account the groove unrelated subchondral bone changes, still the subchondral bone resembles a more sclerotic structure 12-weeks post-surgery as seen in human OA.<sup>42</sup> However, other preclinical animal models showed a decrease of trabecular bone volume and thinning of the subchondral plate.<sup>23</sup> As the subchondral bone remodeling in preclinical animal models might be biphasic, an early decrease in trabecular bone volume followed by a phase in which the subchondral bone becomes denser and stiffens.<sup>23</sup>

Whether the bone remodeling in our study already passed the phase of decrease in trabecular bone volume or directly went to the phase where the bone becomes more sclerotic is unknown.

In contrast to the canine groove model, where small osteophytes are observed at 20-weeks post-surgery,<sup>40</sup> no osteophyte formation is detected in the grooved rat knee joints up to 12-weeks post-surgery. The canine groove model did result in mild inflammation, possibly being responsible for the small osteophytes formed.<sup>19,21,22</sup> As synovial macrophages derived cytokines are assumed to play a role in osteophyte formation in mice,<sup>43</sup> it was suggested that a local inflammatory response is a pre-requisite for osteophyte formation. The joint inflammation observed in the grooved rat knee joints was only minimal or even absent, consequently not resulting in any osteophyte formation.

The groove model in the rat adds to the existing animal models of OA with features resembling (early) human OA. An important distinction is that despite the minimal or even absent synovial inflammation, the degenerative changes are progressive. Because of this, evaluation of cartilage protective effects of treatment is not hampered by inflammatory activity in the joint. This phenomenon makes the groove model especially suitable for evaluation of disease modifying osteoarthritic drugs. A second point of distinction is that there is no permanent trigger causing joint damage, which should render the model more sensitive to treatment. A persistent trigger for joint damage, such as joint instability used in the ACLT models, could counteract the possible beneficial effects of treatment. Moreover, assuming that cartilage repair is possible, the trigger, intrinsic to the cartilage damage itself, could be removed by treatment. Thus, the groove model might be suitable in long term OA progression monitoring after treatment is stopped, and may even be amenable demonstrating a cure.

In conclusion, this is the first time that the groove model has been applied to the tibia-femoral compartment of a rat knee joint. Animal models are essential in research on OA aimed at better understanding of the pathophysiology of OA especially in its early phases and to study the effects and mechanisms of treatment. The groove model of OA in the rat may have an additional value in this respect, as inducing grooves on the articular cartilage of the femoral condyles in the rat results in mild knee joint degeneration of the whole joint already 6 weeks post-surgery. This model can help us better understand the pathophysiology of OA especially in its early phases.

#### AUTHORS' CONTRIBUTIONS

All authors have substantially contributed to the work presented in this paper. All authors contributed to the design, acquisition of data, or analysis and interpretation of data. Finally, all authors have read and approved the final version of the manuscript.

## ACKNOWLEDGMENTS

The research leading to these results has received partial funding from the European Union Seventh Framework Programme (FP7/2007–2013) under grant agreement n°305815. Also supported by the Dutch Arthritis Foundation (LLP-22) and Health–Holland. The funding sources had no role in the study design, collection, analysis, or interpretation of the data; in the writing of the manuscript or in the decision to submit the manuscript for publication.

## REFERENCES

1. Bijlsma JW, Berenbaum F, Lafeber FP. 2011. Osteoarthritis: an update with relevance for clinical practice. *Lancet* 377:2115–2126.
2. Dieppe PA, Lohmander LS. 2005. Pathogenesis and management of pain in osteoarthritis. *Lancet* 365:965–973.
3. Felson DT, Lawrence RC, Dieppe PA, et al. 2000. Osteoarthritis: new insights. Part 1: the disease and its risk factors. *Ann Intern Med* 133:635–646.
4. Buckwalter JA, Martin J, Mankin HJ. 2000. Synovial joint degeneration and the syndrome of osteoarthritis. *Instr Course Lect* 49:481–489.
5. Qvist P, Bay-Jensen AC, Christiansen C, et al. 2008. The disease modifying osteoarthritis drug (DMOAD): is it in the horizon? *Pharmacol Res* 58:1–7.
6. Lotz M, Martel-Pelletier J, Christiansen C, et al. 2013. Value of biomarkers in osteoarthritis: current status and perspectives. *Ann Rheum Dis* 72:1756–1763.
7. Bendele AM, Hulman JF. 1988. Spontaneous cartilage degeneration in guinea pigs. *Arthritis Rheum* 31:561–565.
8. Helminen HJ, Kiraly K, Pelttari A, et al. 1993. An inbred line of transgenic mice expressing an internally deleted gene for type II procollagen (COL2A1). Young mice have a variable phenotype of a chondrodysplasia and older mice have osteoarthritic changes in joints. *J Clin Invest* 92:582–595.
9. Fassler R, Schnegelsberg PN, Dausman J, et al. 1994. Mice lacking alpha 1 (IX) collagen develop noninflammatory degenerative joint disease. *Proc Natl Acad Sci USA* 91:5070–5074.
10. Bendele AM. 2001. Animal models of osteoarthritis. *J Musculoskelet Neuronal Interact* 1:363–376.
11. Teeple E, Jay GD, Elsaid KA, et al. 2013. Animal models of osteoarthritis: challenges of model selection and analysis. *AAPS J* 15:438–446.
12. Gerwin N, Bendele AM, Glasson S, et al. 2010. The OARSI histopathology initiative—recommendations for histological assessments of osteoarthritis in the rat. *Osteoarthritis Cartilage* 18:S24–S34.
13. Janusz MJ, Bendele AM, Brown KK, et al. 2002. Induction of osteoarthritis in the rat by surgical tear of the meniscus: inhibition of joint damage by a matrix metalloproteinase inhibitor. *Osteoarthritis Cartilage* 10:785–791.
14. Hayami T, Pickarski M, Zhuo Y, et al. 2006. Characterization of articular cartilage and subchondral bone changes in the rat anterior cruciate ligament transection and meniscectomized models of osteoarthritis. *Bone* 38:234–243.
15. Karahan S, Kincaid SA, Kammermann JR, et al. 2001. Evaluation of the rat stifle joint after transection of the cranial cruciate ligament and partial medial meniscectomy. *Comp Med* 51:504–512.
16. Guingamp C, Gegout-Pottie P, Philippe L, et al. 1997. Monoiodoacetate-induced experimental osteoarthritis: a dose-response study of loss of mobility, morphology, and biochemistry. *Arthritis Rheum* 40:1670–1679.
17. Tang Z, Yang L, Wang Y, et al. 2009. Contributions of different intraarticular tissues to the acute phase elevation of synovial fluid MMP-2 following rat ACL rupture. *J Orthop Res* 27:243–248.
18. Iijima H, Aoyama T, Ito A, et al. 2014. Destabilization of the medial meniscus leads to subchondral bone defects and site-specific cartilage degeneration in an experimental rat model. *Osteoarthritis Cartilage* 22:1036–1043.
19. Marijnissen AC, van Roermund PM, TeKoppele JM, et al. 2002. The canine ‘groove’ model, compared with the ACLT model of osteoarthritis. *Osteoarthritis Cartilage* 10:145–155.
20. Mastbergen SC, Pollmeier M, Fischer L, et al. 2008. The groove model of osteoarthritis applied to the ovine fetlock joint. *Osteoarthritis Cartilage* 16:919–928.
21. Marijnissen AC, van Roermund PM, Verzijl N, et al. 2002. Steady progression of osteoarthritic features in the canine groove model. *Osteoarthritis Cartilage* 10:282–289.
22. Mastbergen SC, Marijnissen AC, Vianen ME, et al. 2006. The canine ‘groove’ model of osteoarthritis is more than simply the expression of surgically applied damage. *Osteoarthritis Cartilage* 14:39–46.
23. Intema F, Sniekers YH, Weinans H, et al. 2010. Similarities and discrepancies in subchondral bone structure in two differently induced canine models of osteoarthritis. *J Bone Miner Res* 25:1650–1657.
24. Intema F, Mastbergen S, Van Rinsum AC, et al. 2010. Cartilage integrity and proteoglycan turnover are comparable in canine experimentally induced and human joint degeneration. *Rheumatol Rep* 2:50–54.
25. Frost-Christensen LN, Mastbergen SC, Vianen ME, et al. 2008. Degeneration, inflammation, regeneration, and pain/disability in dogs following destabilization or articular cartilage grooving of the stifle joint. *Osteoarthritis Cartilage* 16:1327–1335.
26. Siebelt M, Waarsing JH, Kops N, et al. 2011. Quantifying osteoarthritic cartilage changes accurately using in vivo microCT arthrography in three etiologically distinct rat models. *J Orthop Res* 29:1788–1794.
27. Anraku Y, Mizuta H, Sei A, et al. 2008. The chondrogenic repair response of undifferentiated mesenchymal cells in rat full-thickness articular cartilage defects. *Osteoarthritis Cartilage* 16:961–964.
28. Yoshioka M, Kubo T, Coutts RD, et al. 1998. Differences in the repair process of longitudinal and transverse injuries of cartilage in the rat knee. *Osteoarthritis Cartilage* 6:66–75.
29. Piscoer TM, Waarsing JH, Kops N, et al. 2008. In vivo imaging of cartilage degeneration using microCT-arthrography. *Osteoarthritis Cartilage* 16:1011–1017.
30. Papacharalampous X, Patsouris E, Mundinger A, et al. 2005. The effect of contrast media on the synovial membrane. *Eur J Radiol* 55:426–430.
31. van Tiel J, Siebelt M, Reijman M, et al. 2016. Quantitative in vivo CT arthrography of the human osteoarthritic knee to estimate cartilage sulphated glycosaminoglycan content: correlation with ex-vivo reference standards. *Osteoarthritis Cartilage*. doi: 10.1016/j.joca.2016.01.137. [Epub ahead of print].
32. Kallioniemi AS, Jurvelin JS, Nieminen MT, et al. 2007. Contrast agent enhanced pQCT of articular cartilage. *Phys Med Biol* 52:1209–1219.
33. Palmer AW, Guldberg RE, Levenston ME. 2006. Analysis of cartilage matrix fixed charge density and three-dimensional morphology via contrast-enhanced microcomputed tomography. *Proc Natl Acad Sci USA* 103:19255–19260.
34. Spataro RF, Katzberg RW, Burgener FA, et al. 1978. Epinephrine enhanced knee arthrography. *Invest Radiol* 13: 286–290.
35. Waarsing JH, Day JS, Weinans H. 2004. An improved segmentation method for in vivo microCT imaging. *J Bone Miner Res* 19:1640–1650.
36. Breinan HA, Hsu HP, Spector M. 2001. Chondral defects in animal models: effects of selected repair proce-

- dures in canines. *Clin Orthop Relat Res* 391 (Suppl): S219–S230.
37. Glasson SS, Chambers MG, Van Den Berg WB, et al. 2010. The OARSI histopathology initiative—recommendations for histological assessments of osteoarthritis in the mouse. *Osteoarthritis Cartilage* 18:S17–S23.
38. Chu CR, Szczodry M, Bruno S. 2010. Animal models for cartilage regeneration and repair. *Tissue Eng Part B Rev* 16:105–115.
39. Brandt KD. 2002. Animal models of osteoarthritis. *Biorheology* 39:221–235.
40. Sniekers YH, Intema F, Lafeber FP, et al. 2008. A role for subchondral bone changes in the process of osteoarthritis; a micro-CT study of two canine models. *BMC Musculoskelet Disord* 9:20.
41. Martin EA, Ritman EL, Turner RT. 2003. Time course of epiphyseal growth plate fusion in rat tibiae. *Bone* 32: 261–267.
42. Chappard C, Peyrin F, Bonnassie A, et al. 2006. Subchondral bone micro-architectural alterations in osteoarthritis: a synchrotron micro-computed tomography study. *Osteoarthritis Cartilage* 14:215–223.
43. Blom AB, van Lent PL, Holthuysen AE, et al. 2004. Synovial lining macrophages mediate osteophyte formation during experimental osteoarthritis. *Osteoarthritis Cartilage* 12:627–635.